


NANO EXPRESS

Open Access



Influence of Group Modification at the Edges of Carbon Quantum Dots on Fluorescent Emission

Ju Tang¹, Jin Zhang^{1*} , Yunfei Zhang¹, Yiming Xiao¹, Yanli Shi¹, Yunhua Chen¹, Lan Ding¹ and Wen Xu^{1,2*}

Abstract

We present a detailed investigation on the effect of functional group modulation at the edges of carbon quantum dots (CQDs) on the fluorescence from the CQDs. The CQDs attached by N, S, and P elements are synthesized via pyrolysis of a mixture of citric acid and $\text{NH}_3\text{H}_2\text{O}$, H_2SO_4 , and H_3PO_4 , respectively. Thus, part of $-\text{COOH}$ at the edges of CQDs can be converted into $-\text{C}=\text{O}$ and functional groups such as $-\text{NH}_2$, $-\text{SO}_2$, $-\text{HSO}_3$, and $-\text{H}_2\text{PO}_4$ can connect to the carbon bonds. We find that the formation of the N/S/P-CQDs can reduce the amount of $-\text{COOH}$ that attaches to the edges of sp^2 -conjugated π -domains located at centers of these CQDs. This effect can result in the reduction of the non-radiative recombination for electronic transition in these CQDs. As a result, the quantum yield (QY) for fluorescence from the CQDs can be efficiently enhanced. We demonstrate experimentally that the QYs for N/S/P-CQDs can reach up to 18.7%, 29.7%, and 10.3%, respectively, in comparison to 9% for these without functional group modulation. This work can provide a practical experimental approach in improving the optical properties of fluorescent CQDs.

Keywords: Carbon quantum dot, Functional group modulation, Fluorescent emission

Background

Carbon quantum dots (CQDs) are emerging nanomaterials [1] with superior fluorescent properties [2] and unique chemical, electronic, and optical properties [3]. In contrast to traditional dye molecules and semiconductor-based quantum dots, the CQDs are not only with the good light resistance and scintillation light bleaching resistance [4] but also with important features such as low toxicity, biocompatibility, low cost, high photostability [5], etc. Hence, the CQDs have been proposed as advanced electronic and optoelectronic materials for application in the areas such as optoelectronic devices [6], energy conversion [7], photocatalysis [8], sensors [9], bio-imaging [10], cell markers [11, 12], and drug delivery [13], to mention but a few. In recent years, the investigation of CQDs has become a hot and fast-growing field of research in scientific and industry communities.

At present, the most popularly employed experimental method for chemical synthesis of the CQDs is via bottom-up approach which can be applied to produce fluorescent CQDs simply, cheaply, and in large-scale quantity. In this method, small molecules of organic compounds or polymers are taken as carbon sources and are dehydrated and carbonized to realize the CQDs. During the preparation of the CQDs, the surface and edge of the CQDs are often attached by some chemical groups such as OH, COOH, C=O, and so on. The presence of these chemical groups can affect greatly the electronic and optical properties of the CQDs. In particular, the fluorescent characteristics of the CQDs depend sensitively on the presence of these groups [14]. From a viewpoint of physics, the chemical groups attached to the surface and edge of the CQDs can induce new kinds of surface and edge states into the CQD systems and, thus, can modify the electronic structure and the corresponding electronic and optical transition channels in the CQDs. In this case, the photoluminescence (PL) from the CQDs can be achieved via

* Correspondence: zhangjin96@aliyun.com; wenxu_issp@aliyun.com
¹School of Physics and Astronomy and Key Laboratory of Quantum Information of Yunnan Province, Yunnan University, Kunming 650091, People's Republic of China
Full list of author information is available at the end of the article

electronic transition between edge states and carbon states such as conjugate π states (or sp^2 area). Thus, the mechanism of the PL emission from CQDs is very much akin to that for photo-induced light emission from impurity states in a doped semiconductor [15] in the following way: (i) the photons can be absorbed via electronic transitions from lower and occupied carbon electronic states to higher and empty states under the action of optical pumping, (ii) the photo-excited electrons can be relaxed into the electronic states in the edge states via non-radiative electronic transition events, and (iii) the PL emission can be achieved via electronic transitions from edge states to the lower carbon electronic states accompanied by the emission of photons. Therefore, the edge electronic states play a role like radiative impurity states in a semiconductor and the electrons can be combined with the holes for the luminescence. Generally, the sp^2 -conjugated π -domains are considered to be as the inherent centers for PL emission [16] and the aromatic sp^2 carbon area of a CQD is surrounded by sp^3 carbon (C–OH) states. Hence, the recombination of electron-hole pairs in the sp^2 area and the electronic transitions among carbon and edge states can promote the PL emission from CQDs [17, 18].

The fluorescent quantum yield (QY) is a key parameter to measure the efficiency of photo-induced light emission from a material or a device, which is defined by the number of photons emitted relative to the number of photons absorbed. In the early years when the CQDs were discovered, the QY for chemically prepared CQDs was quite low (even less than 2%) [1]. How to improve the fluorescent QY for CQDs has been a central problem for fundamental research and for material application. In general, the QY for CQDs realized chemically via a bottom-up approach depends on the choice of the carbon source, synthesis technique, and edge modulation. More specifically, the intensity and frequency of the PL emission from CQDs are the consequences of the sample parameters of the CQDs, the presence of the functional groups or edge states, the interaction between electronic states in sp^2 -conjugated π -domains and in chemical groups, and the properties of the fluorophore in the CQDs [19]. In recent years, the fluorescent QY for CQDs has been largely improved [20]. Particularly, Lingam et al. examined the effect of the edge states induced in the synthesis of CQDs on the PL emission. They found that if the edges of the CQDs are damaged, the PL emission drops sharply to be even immeasurable [21]. A similar work by Kumar et al. has also demonstrated that the presence of the edge states is the key factor for PL from CQDs, and the origin of tunable heterogeneous PL is amino-

functionalized for CQDs [22]. Tang et al. reported a simple microwave-assisted hydrothermal synthesis of the CQDs using glucose as the sole carbon source [23]. By simply extending the reaction time from 1 min to 9 min, they could adjust the size of the CQDs from 1.65 nm to 21 nm. Interestingly, they found that the PL from the CQDs was independent upon the size of the CQDs, where the CQDs with the sizes of 9.6 nm and 20 nm show roughly the same light absorption and emission behaviors. The results obtained from further research work by Lin et al. also indicate that the PL emission from CQDs depends weakly on the effect of quantum confinement of the sp^2 -conjugated π -domains [24] and the presence of the surface functional groups attached to the CQDs is the key factor for PL emission. Dong et al. realized the blue fluorescent CQDs with the disc-like nanosheets (the size of 15 nm and the thickness of 0.5–2.0 nm) by adjusting the degree of the carbonation of citric acid. They found that the PL of CQDs is independent on the excitation wavelength and the fluorescent QY can be up to 9.0% [25]. It should be noted that according to the relationship between the size of a CQD and the wavelength of the PL emission for a bare CQD [26], the CQDs with the size of about 2.25 nm can emit the blue fluorescence, while the CQDs with the size of 15 nm can only emit longer wavelength fluorescence. The strong blue PL emission from CQDs with the size of 15 nm [25] suggests once more that the presence of the edge states induced by chemical groups attached to the CQDs is mainly responsible for PL emission from CQDs. Therefore, the edge functionality of the CQDs can affect not only the fluorescence of CQDs, but also the physical and chemical properties of the CQDs in general [19].

It should be noticed that at present, the frequency of the fluorescent emission from CQDs cannot be easily controlled and modified artificially. Furthermore, the corresponding fluorescent QY has not yet reached the requirements for the application as practical devices. The results obtained from experimental [27–29] and theoretical [30, 33] research have confirmed that the edge passivation can effectively improve the electronic optical properties of CQDs. Passivation agents are widely used to adjust the fluorescent properties of CQDs [21–23]. Jing Liu et al. developed a one-step preparation of nitrogen-doped and surface-passivated carbon quantum dots [27]. They found that the QY of CQDs without surface passivation is usually quite low (QY < 10%), passivated CQDs show a QY of 37.4%. A similar work by Shen et al. researched the PEG-passivated CQDs have a QY of 28% [28], and Kwon et al. reported that hexadecyl amine (HDA)-passivated one yields 19–35% [29].

Dimos and co-workers also found that the edge passivation can effectively induce the electrons in the conduction band and increase the surface energy of the CQDs to prevent fluorescence decay or quenching caused by the aggregation of CQDs [30]. Furthermore, the fluorescent generation from CQDs fabricated via chemical reaction or bottom-up approach is mainly induced by the presence of the radiative functional groups or fluorophore attached to the edge of the CQDs [31]. Chemically, these functional groups can be modified via putting the CQDs into different chemical solutions. The fluorescence of these chemically modified CQDs can be achieved via the excitonic emission accompanied by electronic recombination and separation of electron-hole pairs trapped on the edge of CQDs [32]. Thus, the frequency of the PL emission can be tuned via selecting different edge groups to form required edge states.

The prime motivation of this study is to explore how the fluorescent properties of the CQDs can be modified in different chemical solutions for their passivation or edge functionality. Recently, we had produced CQDs from tofu wastewater without adding any toxic substances and revealed the luminescence mechanism [33]. We found that different colors of the fluorescent emission from these CQDs can be achieved via putting these dot materials in water or in NaOH solution [33]. We had also fabricated the CQDs from fresh lemon juice and applied them for cellular imaging [34]. It was found that the presence of oxygen-containing groups on the surface and edge of the CQDs is mainly responsible for the fluorescence of the CQDs [34]. Our attention of the present study is mainly focused on how to achieve an effective way in improving the quantum yield of fluorescence from CQDs.

Method

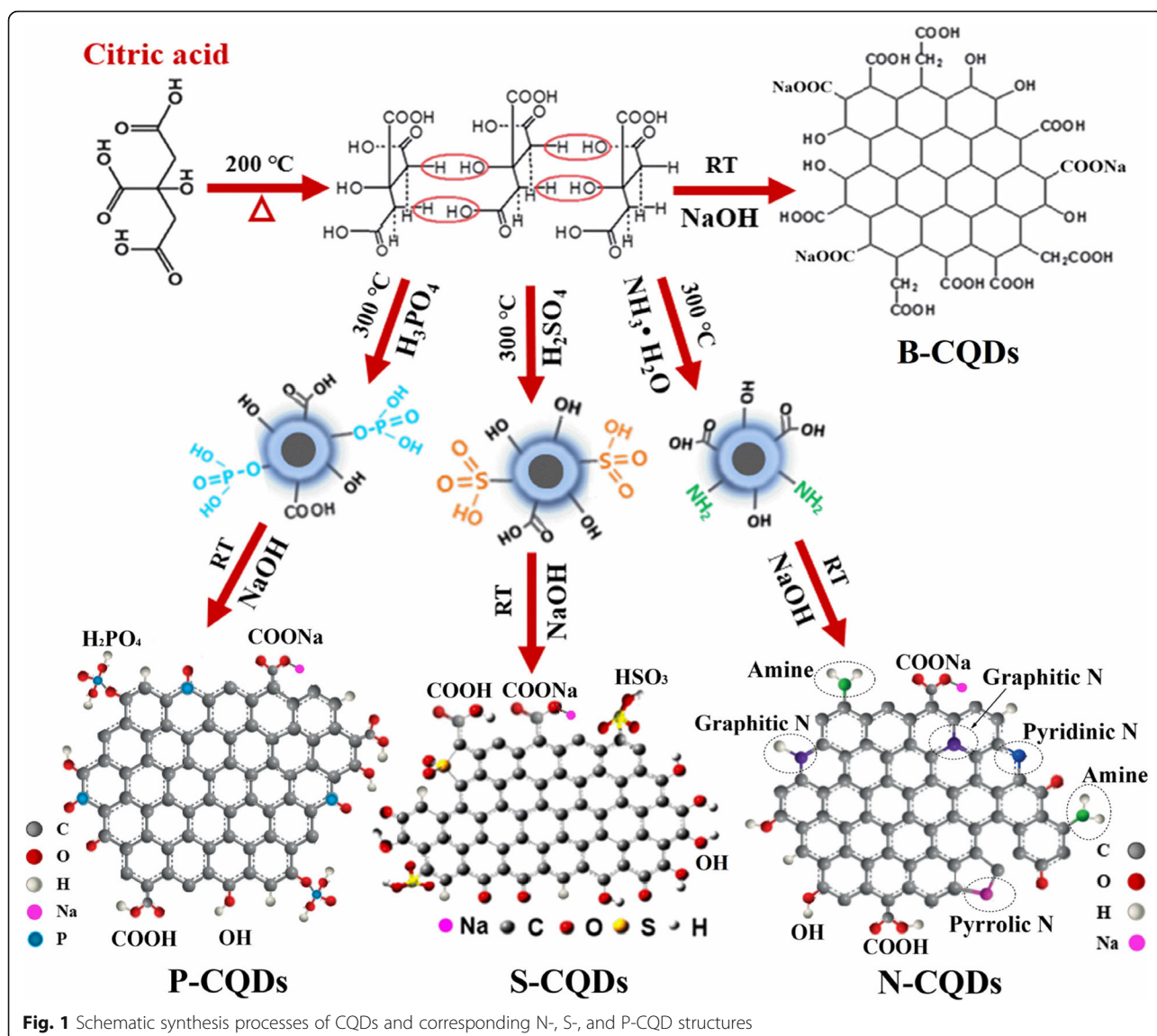
Synthesis of N-, S-, and P-CQDs

In this work, citric acid ($C_6H_8O_7$, 99.5%), sodium hydroxide (NaOH, 96%), ammonia solution (NH_3 H_2O , 25–28%), sulfuric acid solution (H_2SO_4 , 98%), phosphoric acid solution (H_3PO_4 , 85%), and deionized water were used to fabricate the CQDs and to modify the edge states.

The B-CQDs were synthesized by pyrolysis of citric acid as sole carbon source. The N/S/P-CQDs were fabricated by pyrolysis of ammonia, sulfuric acid, and phosphoric acid together with citric acid, respectively. The principle and the experimental processes for the realization of the CQDs and corresponding N/S/P-CQDs are shown in Fig. 1. Through the pyrolysis of the citric acid, the B-CQDs can be fabricated via inter-molecular dehydration, carbonization, and condensation reaction.

This approach can form (i) the aromatic structure (namely the sp^2 carbon states with C–C and C=C bonds) with conjugate area as the core of the CQDs, (ii) the edges of the CQDs attached by hydroxyl (OH) and carboxyl ($COOH/-O-C=O$), and (iii) the sp^3 carbon (C–C–OH/–C–O) area which can be passivated in, e.g., NaOH solution. The N-CQDs can be achieved via pyrolysis process of the mixed solution of citric acid and NH_3H_2O . In such a case, the dehydrogenation reaction among adjacent groups with carboxyl can promote the formation of pyrrolic N in graphene skeleton of the CQDs. The edges of the N-CQDs are then attached with extra chemical groups such as –C–N and $-NH_2$ [35]. Similar to the realization of the N-CQDs, S-CQDs, and P-CQDs can be fabricated via the pyrolysis of the mixed solution of citric acid and H_2SO_4 and H_3PO_4 , respectively. The inter-molecular dehydration, carbonization, and condensation reaction can form graphene skeleton of the CQDs with the connection to chemical groups such as $-SO_2$, $-HSO_3$, and $-H_2PO_4$. Furthermore, S and P atoms are likely to attach to the edge of sp^2 carbon conjugate area to form the edge defects. The material structures of N/S/P-CQDs are shown in Fig. 1. In the present study, N/S/P-CQDs are dispersed in NaOH solution at room temperature to make them passivation. Thus, we can convert part of the $-COOH$ at the edge of the CQDs into $-COONa$ and reduce the amount of $-COOH$ at the edge of sp^2 -conjugated π -domains. Consequently, the group modification at the edge of the CQDs can be achieved.

More specifically, the fluorescent N/S/P-CQDs are prepared in the following ways: (i) 2 g analytically pure citric acid was added into 60 ml NH_3H_2O (pH = 7.5), 60 ml H_2SO_4 (pH = 3), and 60 ml H_3PO_4 (pH = 3), respectively. (ii) We place the mixed solution onto the heating platform for constant heating at 300 °C, where the heating time is for 20–30 min. (iii) 50 ml sodium hydroxide solution (NaOH) is added into the beaker after the beaker cooling down naturally till room temperature. (iv) The mixture is magnetically stirred for 10 min and ultrasonically shocked for 10 min and further centrifuged at a speed of 12,000 r/min for 10–30 min. Then, the supernatant is taken, in which N/S/P-CQDs modified by ammonia, sulfuric acid, and phosphoric acid solutions, respectively, and passivated by groups such as $-OH$, $-COOH$, $-C=O$, $-COONa$, $-NH_2$, $-SO_2$, $-HSO_3$, and $-H_2PO_4$ can be obtained in NaOH solutions. In the preparation of N/S/P-CQDs, except that the N/S/P-CQDs were modified by NH_3H_2O , H_2SO_4 , and H_3PO_4 , respectively, the other experimental conditions were roughly the same. We used the same amount of citric acid to dissolve into NH_3H_2O , H_2SO_4 , and H_3PO_4 , respectively, for pyrolysis



and then added the same amount and equal concentration of sodium hydroxide solution when the substances in the beaker were almost dry. This can ensure that the density of the CQDs in NaOH solution is almost the same.

Measurements

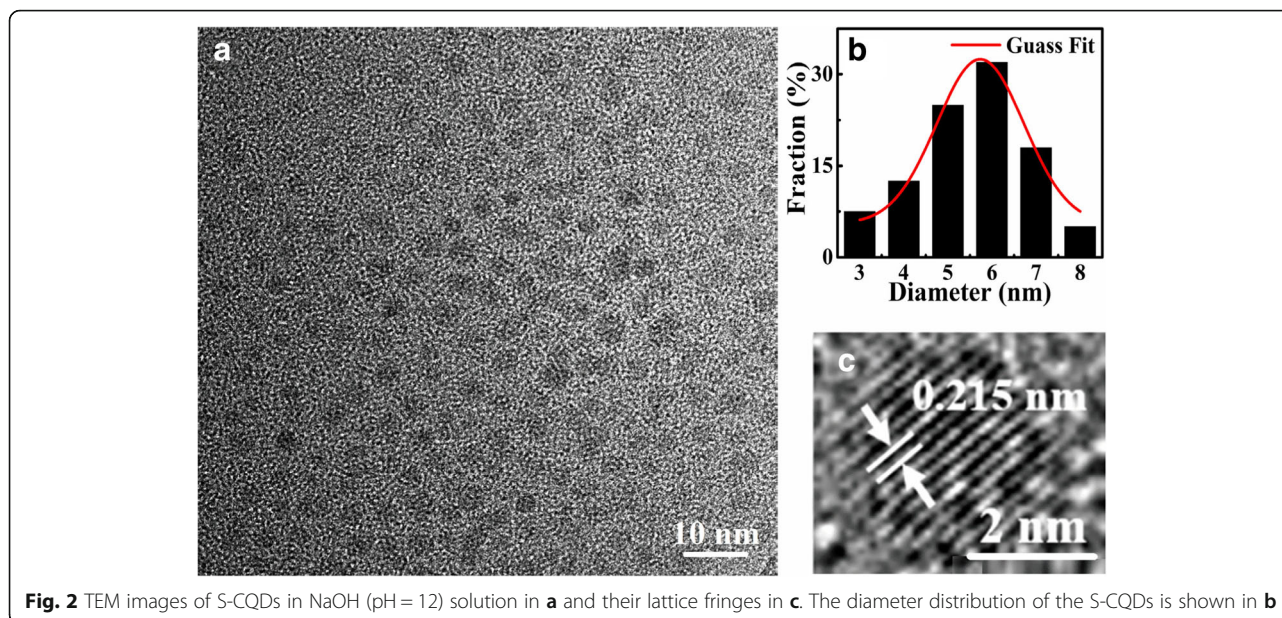
In this work, the morphology and microstructure of the CQDs were observed by using the transmission electron microscopy (TEM, JEM 2100) at an accelerating voltage of 300 kV. The X-ray photoelectron spectroscopy (XPS) was applied to characterize the samples, by using PHI5000 Versa Probe II photoelectron spectrometer with Al K α at 1486.6 eV. The ultraviolet-visible (UV-Vis) absorption spectrum of the CQDs was measured by a UV-Vis spectrophotometer (Specord200, Germany). The PL emission from the CQDs was measured using a

standard PL system (IHR320, Jobin Yvon, USA) at room temperature. The fluorescent QY of the CQDs is evaluated on the base of the PL data.

Results and Discussions

The Characterization of Samples

The morphology and structures of as-synthesized CQDs were investigated by TEM. Figure 2 shows the TEM images (a) and the diameter distributions (b) of S-CQDs. It can be clearly seen that the S-CQDs are circular-like sheets and are dispersed uniformly in NaOH solution. Through a statistical average of the TEM images for the CQDs, we find that the size distribution of S-CQDs is mainly located in 3–8-nm range and the average size of the CQDs is about 5.73 nm. These results are obtained by statistical analysis of more than 300 CQD particles using the Image J

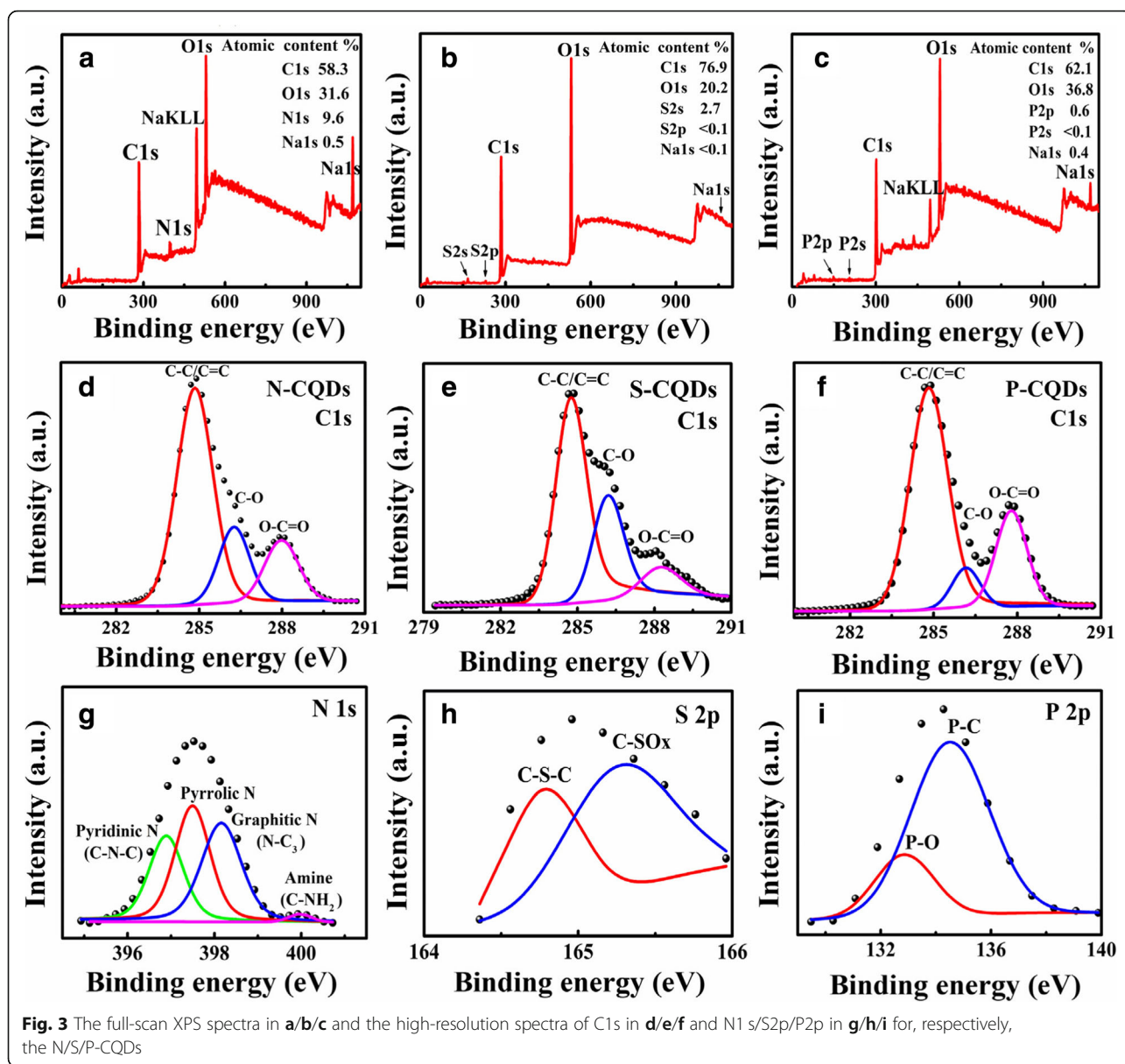


software. The results shown in Fig. 2 c indicate that these S-CQDs are highly crystallized with typical lattice structure of carbon. The lattice fringes of the CQDs are clear and the corresponding lattice spacing is about 0.215 nm consistent with the (100) facet of graphene [32].

In the present study, we apply the X-ray photoelectron spectroscopy (XPS) for the measurement and examination of the edge functional groups attached to the CQDs. We use glass sheets as the substrates and coat the samples on the glass sheets for the measurements. In Fig. 3, we show the XPS spectra for N-, S- and P-CQDs. As shown in Fig. 3 a, the full-scan XPS spectrum for N-CQDs indicates that the atomic percentage of N1s is 9.6%. Figure 3 b and c indicate that (i) the S- and P-CQDs show response peaks for S2s (at 169 eV) and P2s (at 133 eV), respectively, in contrast to CQDs prepared without functional group modification and (ii) the atomic percentages of S2s for S-CQDs and of P2p for P-CQDs are 2.7% and 0.6%, respectively. The main reason for a lower content of P in P-CQDs than S content in S-CQDs is that P has a relatively larger atomic radius (proton number of nuclei is 15) than S has (proton number of nuclei is 16). Thus, P atoms are relatively less likely to be absorbed by the chemical bonds on the surface of CQDs than S atoms are. In comparison with Fig. 3 a and c for the XPS spectra for N- and P-CQDs, Fig. 3 b shows that the percentage of C1s atoms in S-CQDs is much higher (76.9%) and the proportions of O1s atoms (20.2%) and impurity atoms (S, Na) are very low. These results indicate that there

are fewer defects in the sp^2 carbon area in S-CQDs. Shown in Fig. 3 d are the high-resolution spectra of C1s exhibits three typical peaks, respectively, at 284.8 eV, 286.6 eV, and 288.5 eV for N-CQDs, which indicate that the sp^2 carbon (C–C/C=C) area has a good lattice structure [14, 25, 36]. Furthermore, sp^3 carbon (C–O/C–N, 286.4 eV) and carboxyl (O–C=O/COOH, 288.1 eV) have similar binding energy [33], suggesting that there are similar amounts of hydroxyl (C–O/C–OH) and carboxyl (O–C=O/COOH) around the sp^2 carbon area. The corresponding high-resolution spectra of C1s for S- and P-CQDs are shown in Fig. 3 e and f. As shown in Fig. 3 e, the peak of sp^3 carbon (C–O) is very strong and the peak of hydroxyl (O–C=O/COOH) is weak for S-CQDs, indicating that the amount of hydroxyl (C–O/C–OH) are much higher than carboxyl (O–C=O/COOH) around the sp^2 carbon area for S-CQDs. In addition, Fig. 3 h indicate that the amount of hydroxyl (C–O/C–OH) is less than carboxyl (O–C=O/COOH) around the sp^2 carbon area for P-CQDs. Comparing with Fig. 3 d, e, and f, we find that the peak of hydroxyls (C–O/C–OH) is the strongest one while the peak of hydroxyls (O–C=O/COOH) is the weakest one for S-CQDs. When the amount of hydroxyl groups is increased, the amount of carboxyl groups is reduced, and vice versa, when the amount of carboxyl groups is increased, the amount of hydroxyl groups is decreased.

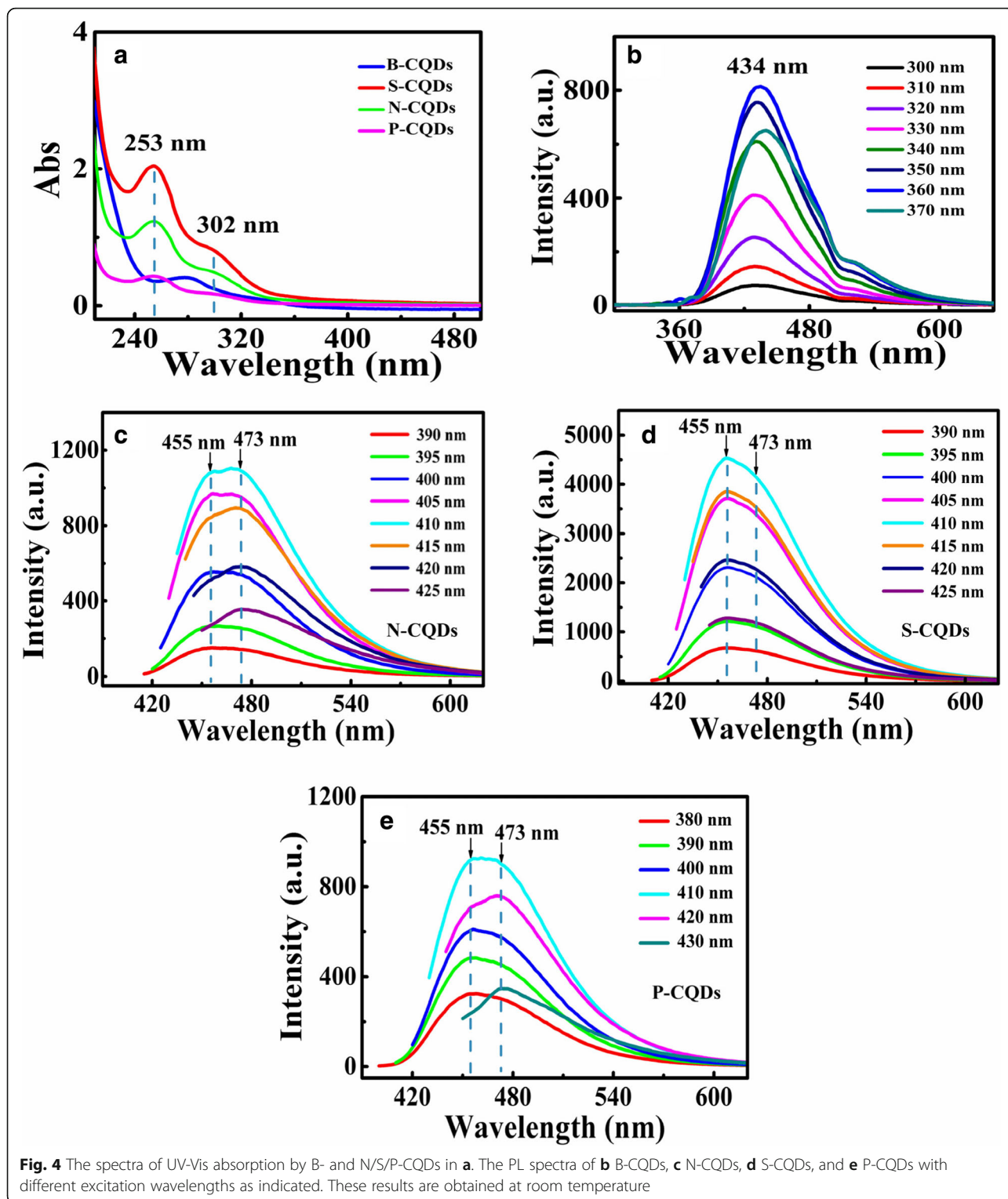
In Fig. 3 g, the high-resolution spectra of N1s show four peaks related to pyridinic nitrogen (pyridinic N, 396.9 eV), pyrrolic nitrogen (pyrrolic N, 397.6 eV),



graphite nitrogen ($N-C_3$, 398.5 eV, located in the center of sp^2 carbon) and the amide group ($C-NH_2$, 399.9 eV, located at the edge of sp^2 carbon), respectively [22, 37–39]. These results verify the material structure of N-CQDs shown in Fig. 1. In N-CQDs, the fluorophores are formed by the hybridization of edge functional groups such as $C-OH$ and $C-NH_2$ with sp^2 -conjugated π -domains [40], which can play a role in enhancing the fluorescence of N-CQDs. The high-resolution spectrum of S2s and P2p corresponding to XPS results for S- and P-CQDs are shown in Fig. 3 h and i, it implies that the edges of S-CQDs and P-CQDs are attached by some chemical bonds such as $C-S-C$ (164.8 eV) [41], $C-SO_X$

($X = 2, 3, 4$, 165.1 eV) [42], $P-C$ (135.0 eV) [43], and $P-O$ (132.7 eV) [44]. Thus, the chemical bonds such as $C-SO_2$, $-HSO_3$, $C-P-C$, $-H_2PO_4$, etc. can be formed at the edges of the S- and P-CQDs, as shown in Fig. 1.

Fig. 4 shows the absorption and emission spectra measured from the B- and N/S/P-CQDs in NaOH solutions. Shown in Fig. 4 a are the UV-Vis absorption spectra of B/N/S/P-CQDs. The absorption spectrum of B-CQDs exhibits UV absorption peaks at 278 nm, while UV-Vis absorption spectrum of N-, S-, and P-CQDs depicts two clear absorption bands. The absorption peak at 253 nm is attributed to $\pi-\pi^*$ transition of aromatic $C=C$ bond and the shoulder at 302 nm corresponds to $n-\pi^*$



transition of C=O bond [40]. The C=C bonds come from sp^2 -conjugated domains in the cores of N/S/P-CQDs, while C=O bonds originate from the numerous electron-withdrawing oxygen-containing groups such as carboxyl

and carbonyl groups existing at the edge sites of N/S/P-CQDs. The two absorption peaks reveal the existence of sp^2 -conjugated structures and oxygen-containing functional groups (C=O and O-C=O/COOH) in N-, S-, and P-CQDs.

Figure 4 b–e show the PL spectra of B- and N/S/P-CQDs. As we can see, the strong PL emission can be observed in these CQDs. We find that the intensity of the PL emission first increases then decreases with increasing excitation wavelength. This effect has been found in most nano-structured materials (see, e.g., Ref. [45]). As has been pointed out by Ref. [38], the dependence of the intensity of the PL emission upon excitation for CQDs is mainly originated due to heterogeneous surface states and the sizes and electronic properties of the heteroatoms. For the case of the CQDs with surface group modulation, the presence of the surface states can alter the band gap and radiative energy states of the CQDs. Under relatively shorter wavelength excitation, the electrons are pumped into higher energy states in conduction band further away from radiative electronic states induced by the surface modulation. Thus, the possibility for photon emission from CQDs is reduced by shorter wavelength excitation. Namely, the intensity of the PL emission increases with excitation wavelength in a shorter wavelength regime. In a relatively long wavelength regime, longer wavelength excitation implies that relatively less electrons can be pumped into the conduction band in CQDs. As a result, the intensity of the PL emission decreases with increasing excitation wavelength in a long excitation wavelength regime. Furthermore, the PL emissions of N/S/P-CQDs consist of two overlapping spectral bands [25]. The double PL peaks can be measured respectively at about 455 nm and 473 nm via 410-nm wavelength excitation. This is a consequence of the PL emissions from N/S/P-CQDs modified by different functional groups to affect the radiative recombination of electron-hole (e-h) pairs formed by sp^2 -conjugated π -domains and edge state groups [32, 40]. The possible mechanism proposed here is that (i) the photo-excitation of electrons in N/S/P-CQDs is achieved via $\pi-\pi^*$ transitions from sp^2 -conjugated π -domains to $n-\pi^*$ transitions, (ii) the electrons are relaxed from $n-\pi^*$ states to C=O energy levels via non-radiative transition channels, and (iii) the radiative recombination for holes in discrete sp^2 -related states and electrons in edge states can be induced by abundant functional groups [46].

In Fig. 4 b–e, under the same experimental conditions, we find that the fluorescence intensity of N/S/P-CQDs were significantly higher than that of B-CQDs. The intensity of PL emission from S-CQDs is the strongest, followed by N-CQDs, and the PL emission from P-CQDs is the weakest. This finding corresponds to the results shown in high-resolution spectra of C1s for N/S/P-CQDs (see Fig. 3d, e, f). The intensity of PL emission increases with increasing the peak height of C–O (C–OH)

and with decreasing the peak height of O–C=O (COOH). Therefore, it is reasonable to believe that N/S/P-CQDs with various edge groups, such as C–OH, COOH, C=O, and C–H, can induce different kinds of edge states and influence the intensity of its photoluminescence. Most interestingly, we find that the peak positions for PL emission from N/S/P-CQDs depend on the excitation wavelength, which implies that the radiative electronic states induced by functional groups attached to the edges of the CQDs are quite stable.

As mentioned above, sp^2 carbon area of S-CQDs has fewer defects so that the inherent light emission from S-CQDs is the strongest, compared with N- and P-CQDs. After using the formula for evaluating the fluorescent quantum yield [33], we obtain that the QYs for N/S/P-CQDs are 18.7%, 29.7%, and 10.3%, respectively. Thus, the largest QY can be achieved for S-CQDs, followed by N- and P-CQDs. As we know, the QY of CQDs is a consequence of competing process between radiative electronic transition and non-radiative traps [32]. The hydroxyl (C–O/C–OH) at the edges of the CQDs can be hybridized synergistically with electronic states in sp^2 -conjugated π -domains to form the fluorophores, while those carboxyl (–COOH) can play a role like non-radiative recombination center at the edge of the CQDs [40]. Therefore, the QY of CQDs is affected by the C–O/C–OH and O–C=O/COOH groups. Moreover, we find that using sulfuric acid for modification of the functional groups at the edge of S-CQDs can affect significantly the enhancement of PL emission from S-CQDs, compared with N- and P-CQDs. The QY of 29.7% for S-CQDs, realized in this study, is larger than 18.7% for N-CQDs, 10.3% for P-CQDs, and 9% for CQDs [23] prepared without ammonia, sulfuric acid, or phosphoric acid.

In this work, the N/S/P-CQDs are synthesized by pyrolysis of these mixtures of citric acid and NH_3H_2O , H_2SO_4 , and H_3PO_4 , subsequently dispersed in the NaOH solutions. It can promote inter-molecular dehydration, carbonization, and condensation reaction for citric acid. Carboxyl (–COOH) at the edges of the CQDs can be converted into carbonyl (–C=O) [19], and the edges of N/S/P-CQDs can be attached by chemical groups such as –OH, –COOH, –C=O, – NH_2 , – SO_2 , – HSO_3 , and – H_2PO_4 . Therefore, the formation of the N/S/P-CQDs can reduce the amount of –COOH attached to the edges of sp^2 -conjugated π -domains and can result in the reduction of non-radiative recombination [47]. Consequently, the fluorescent QY of CQDs can be efficiently enhanced.

Conclusions

In this study, we have developed an effective experimental method to enhance the fluorescent quantum yield of

CQDs. N/S/P-CQDs have been synthesized by pyrolysis citric acid and using, respectively, ammonia, sulfuric acid, and phosphoric acid for edge group modifications. The results have shown that the presence of the edge functional groups can play a significant role in generating and enhancing the fluorescence from these CQDs. Especially, the hydroxyl (C–O/C–OH) groups at the edges of sp^2 -conjugated π -domains can affect significantly the fluorescent quantum yields of the CQDs. Nevertheless, the attachment of carboxyl (O–C=O/–COOH) groups to the edges of sp^2 -conjugated π -domains leads mainly to non-radiative recombination centers, which can weaken the PL emission from the CQDs. In the present study, the QYs for N/S/P-CQDs can reach up to 18.7%, 29.7%, and 10.3%, respectively. These values are much higher than that of 9% for CQDs prepared without functional group modification. The most important conclusion we draw from this study is that the group modification at the edges of the CQDs by sulfuric acid can affect strongly the fluorescence emission and QY of the CQDs.

Abbreviations

CQDs: Carbon quantum dots; PL: Photoluminescence; QY: Quantum yield; TEM: Transmission electron microscope; UV-Vis: Ultraviolet visible; XPS: X-ray photoelectron spectroscopy; XRD: X-ray diffraction

Acknowledgements

We thank Prof X.K. Yang from the Kunming University of Science and Technology for the helpful discussions about the results obtained from XPS measurements.

Authors' Contributions

JT fabricated the samples, carried out the sample characterization, part of XPS measurement, and prepared the presentation materials for the manuscript. JZ proposed the research work and carried out the analyses of the experimental results. YFZ fabricated the samples and took part in the sample characterization, UV-Vis, and XPS measurements. YMX participated in the preparation of the manuscript. YLS undertook the analyses of the experimental results. YHC participated in the fabrication of samples. LD conducted part of the PL measurement of the samples. WX participated in the analyses of the experimental results and in the revision of the manuscript. All authors read and approved the final manuscript.

Authors' Information

JT is a Ph.D., JZ is a Professor, YFZ is a post-graduate student, YMX is a Lecturer, YLS is a Professor, and YHC and LD are an Associate Professor at Yunnan University. WX is a Professor at Yunnan University and a Professor at the Institute of Solid State Physics, Chinese Academy of Sciences.

Funding

This work was supported by the National Natural Science Foundation of China (grant Nos. 11664044, 11364045, 11574319, U1832153), the Department of Science and Technology of Yunnan Province (grant Nos. 2016FC001, 2015FA040), Yunnan University (grant No. 2016MS14), and the Center of Science and Technology of Hefei Academy of Science (2016FXZY002)

Availability of Data and Materials

The datasets generated during and/or analyzed during the current study are available from the corresponding authors on reasonable request.

Competing Interests

The authors declare that they have no competing interests.

Author details

¹School of Physics and Astronomy and Key Laboratory of Quantum Information of Yunnan Province, Yunnan University, Kunming 650091, People's Republic of China. ²Key Laboratory of Materials Physics, Institute of Solid State Physics, Chinese Academy of Sciences, Hefei 230031, People's Republic of China.

Received: 14 May 2019 Accepted: 7 July 2019

Published online: 02 September 2019

References

- Xu X, Ray R, Gu Y et al (2004) Electrophoretic analysis and purification of fluorescent single-walled carbon nanotube fragments. *Journal of the American Chemical Society* 126(40):12736–12737
- Sun YP, Zhou B, Lin Y et al (2006) Quantum-sized carbon dots for bright and colorful photoluminescence. *Journal of the American Chemical Society* 128(24):7756–7757
- Novoselov KS, Geim AK, Morozov SV et al (2004) Electric field effect in atomically thin carbon films. *Science* 306(5696):666–669
- Ding Y, Zhang F, Xu J et al (2017) Synthesis of short-chain passivated carbon quantum dots as the light emitting layer towards electroluminescence. *RSC Adv* 7:28754–28762
- Chen Z, Wang X, Li H, Li C, Lu Q, Yang G, Long J, Meng L (2015) Controllable and mass fabrication of highly luminescent N-doped carbon dots for bioimaging applications. *RSC Adv* 5:22343–22349
- Bourlinos AB, Stassinopoulos A et al (2008) Surface functionalized carbon genic quantum dots. *Small No.* 4:455–458
- Wang Z, Yuan F, Li X, Li Y, Zhong H, Fan L, Yang S (2017) 53% efficient red emissive carbon quantum dots for high color rendering and stable warm white-light emitting diodes. *Adv. Mater* 29:1702910
- Wang F, Liu C-y (2011) White light-emitting devices based on carbon dots electroluminescence. *Chem Commun* 47:3502–3504
- Wang K, Gao ZC, Gao G et al (2013) Systematic safety evaluation on photo luminescent carbon dots. *Nanoscale Res Lett.* 8:122–130
- Bhunia SK, Saha A, Maity AR, Ray SC, Jana NR (2013) Carbon nanoparticle-based fluorescent bioimaging probes. *Scientific Reports* volume 3:1473
- Tao H, Yang K, Ma Z, Wan J, Zhang Y, Kang Z, Liu Z (2013) In vivo NIR fluorescence imaging, biodistribution, and toxicology of photoluminescent carbon dots produced from carbon nanotubes and graphite. *Small* 2:281–290
- Wu ZL, Zhang P, Gao MX et al (2013) One-pot hydrothermal synthesis of highly luminescent nitrogen-doped amphoteric carbon dots for bioimaging from Bombyx moil silk-natural proteins. *J Mater Chem B* 1(22):2868–2873
- Bhunia SK, Pradhan N, Jana NR (2014) Vitamin B1 derived blue and green fluorescent carbon nanoparticles for cell-imaging application. *ACS Appl Mater Interfaces* 6(10):7672–7679
- Mondal TK, Gupta A, Shaw BK et al (2016) Highly luminescent N-doped carbon quantum dots from lemon juice with porphyrin-like structures surrounded by graphitic network for sensing applications. *RSC Adv* 6:59927
- Ajimsha RS, Anoop G, Aravind A et al (2008) Luminescence from surfactant-free ZnO quantum dots prepared by laser ablation in liquid. *Electrochemical and Solid-State Letters* 11(2):K14–K17
- Chien C-T, Li S-S, Lai W-J et al (2012) Tunable photoluminescence from graphene oxide. *Angew. Chem. Int. Ed* 51:6662–6666
- Zhu S, Tang S, Zhang J, Yang B (2012) Control the size and surface chemistry of graphene for the rising fluorescent materials. *Chem. Commun.* 48:4527–4539
- Wilson WL, Szajowski PF, Brus LE (1993) Quantum confinement in size-selected, surface-oxidized silicon nanocrystals. *Science* 262:1242–1244
- Dan Q, Zheng M, Zhang L, Zhao H et al (2014) Formation mechanism and optimization of highly luminescent N-doped graphene quantum dots. *Sci. Rep* 4:5294
- Chen C-F, Park C-H, Boudouris BW et al (2011) Controlling inelastic light scattering quantum pathways in graphene. *Nature* 471:617–620
- Lingam K, Podila R, Qian H et al (2013) Evidence for edge-state photoluminescence in graphene quantum dots. *Adv. Funct. Mater* 23: 5062–5065
- G. Sandeep Kumar, Rajarshi Roy, Dipayan Sen, Uttam K. Ghorai et al (2014) Amino-functionalized graphene quantum dots: origin of tunable heterogeneous photoluminescence. *Nanoscale* 6: 3384–3391

23. Tang L, Ji R, Cao X, Lin J, Jiang H, Li X et al (2012) Deep ultraviolet photoluminescence of water-soluble self-passivated graphene quantum dots. *ACS Nano*. 6(6):5102–5110
24. Lin L, Zhang S et al (2012) Creating high yield water soluble luminescent graphene quantum dots via exfoliating and disintegrating carbon nanotubes and graphite flakes. *Chem. Commun.* 48:10177–10179
25. Dong Y, Shao J, Chen C et al (2012) Blue luminescent graphene quantum dots and graphene oxide prepared by tuning the carbonization degree of citric acid. *Carbon* 50:4738–4743
26. Eda G, Lin Y-Y, Mattevi C et al (2010) Blue photoluminescence from chemically derived graphene oxide. *Adv. Mater.* 22:505–509
27. Liu J, Luo XLH et al (2014) One-step preparation of nitrogen-doped and surface-passivated carbon quantum dots with high quantum yield and excellent optical properties. *RSC Adv.* 4:7648
28. Shen Y, Zhu X, Yang J, Zong JZ et al (2012) One-pot hydrothermal synthesis of graphene quantum dots surface-passivated by polyethylene glycol and their photoelectric conversion under near-infrared light. *New J. Chem.* 36:97–101
29. Kwon W, Rhee SW (2012) Facile synthesis of graphitic carbon quantum dots with size tunability and uniformity using reverse micelles. *Chem. Commun* 48:5256–5258
30. Dimos K (2016) Carbon quantum dots: surface passivation and functionalization. *Current Organic Chemistry* 14:682–695(14)
31. Huili F, Ji Z, Chen X, Cheng A et al (2017) A versatile ratiometric nanosensing approach for sensitive and accurate detection of Hg^{2+} and biological thiols based on new fluorescent carbon quantum dots. *Analytical and bioanalytical chemistry* 409:2373–2382
32. Yuan F, Yuan T, Sui L et al (2018) Engineering triangular carbon quantum dots with unprecedented narrow bandwidth emission for multicolored LEDs. *Nature Communications*. 9:2249
33. Zhang J, Wang H, Xiao Y, Tang J, Liang C, Li F, Dong H, Xu W (2017) A simple approach for synthesizing of fluorescent carbon quantum dots from tofu wastewater. *Nanoscale Research Letters* 12:611
34. He M, Zhang J, Wang H, Kong Y, Xiao Y, Xu W (2018) Material and optical properties of fluorescent carbon quantum dots fabricated from lemon juice via hydrothermal reaction. *Nanoscale Research Letters* 13:175
35. Peng J, Gao W, Gupta BK et al (2012) Graphene quantum dots derived from carbon fibers. *Nano Lett* 12:844–849
36. Zhu S, Zhang J, Tang S et al (2012) Surface chemistry routes to modulate the photoluminescence of graphene quantum dots: from fluorescence mechanism to up-conversion bioimaging applications. *Adv. Funct. Mater* 22: 4732–4740
37. Niino S, Takeshita S, Iso Y, Isobe T (2016) Influence of chemical states of doped nitrogen on photoluminescence intensity of hydrothermally synthesized carbon dots. *Journal of Luminescence* 180:123–131
38. Singh VK, Singh V, Yadav PK et al (2018) Bright-blue-emission nitrogen and phosphorus-doped carbon quantum dots as a promising nanoprobe for detection of Cr(VI) and ascorbic acid in pure aqueous solution and in living cells. *New J.Chem.* 42:12990
39. Song Z, Quan F, Xu Y, Liu M, Liang C, Liu J (2016) Multifunctional N, S co-doped carbon quantum dots with pH- and thermo-dependent switchable fluorescent properties and highly selective detection of glutathione. *Carbon*. 104:169–178
40. Zhu S, Song Y, Zhao X, Shao J, Zhang J, Yang B (2015) The photoluminescence mechanism in carbon dots (graphene quantum dots, carbon nanodots, and polymer dots): current state and future perspective. *Nano Research* 8(2):35–381
41. Yang YH, Cui JH, Zheng MT, Hu CF, Tan SZ, Xiao Y et al (2012) One step synthesis of amino-functionalized fluorescent carbon nanoparticles by hydrothermal carbonization of chitosan. *Chem Commun.* 48(3):380–382
42. Li Y, Wang J, Li X et al (2012) Discharge product morphology and increased charge performance of lithium-oxygen batteries with graphene nanosheet electrodes: the effect of sulphur doping. *Mater. Chem* 22:20170–20174
43. Han Y, Tang D, Yang Y et al (2015) Non-metal single/dual doped carbon quantum dots: a general flame synthetic method and electro-catalytic properties. *Nanoscale*. 7(14):5955–5962
44. Zhang F, Feng X, Zhang Y et al (2013) Photoluminescent carbon quantum dots as directly film-forming phosphor towards white LEDs. *Nanoscale* 00:1–3
45. Li C, Ding L, Liang C, Zhang J, Zhang C, Mei H et al (2017) Photon-induced light emission from foamed gold with micro/ nanohollow sphere structures. *ACS Omega* 2:5759–5765
46. Xu Q, Zhou Q, Zheng H, Xue Q et al (2013) Single-particle spectroscopic measurements of fluorescent graphene quantum dots. *ACS Nano* 7:10654–10661
47. Mei Q, Zhang Z (2012) Photoluminescent graphene oxide ink to print sensors onto microporous membranes for versatile visualization bioassays. *Angew. Chem. Int. Ed* 51:5602–5606

Publisher's Note

Springer Nature remains neutral with regard to jurisdictional claims in published maps and institutional affiliations.

Submit your manuscript to a SpringerOpen[®] journal and benefit from:

- Convenient online submission
- Rigorous peer review
- Open access: articles freely available online
- High visibility within the field
- Retaining the copyright to your article

Submit your next manuscript at ► [springeropen.com](https://www.springeropen.com)
